Effect of Macrostructural Control of an Auxiliary Layer on the CO_2 Sensing Properties of NASICON-based Gas Sensors

Masataka Morio[a], Takeo Hyodo[a], Yasuhiro Shimizu[b,*], and Makoto Egashira[b]

[a]*Graduate School of Science and Technology, Nagasaki University*

[b]*Fuculty of Engineering, Nagasaki University*

1-14 Bunkyo-machi, Nagasaki 852-8521, Japan

**E-mail: shimizu@nagasaki-u.ac.jp*

Abstract

Macrostructural effects of an auxiliary electrode on the CO_2 gas sensing properties of NASICON ($Na_3Zr_2Si_2PO_{12}$) solid electrolyte sensors were investigated. The sensor with a porous Li_2CO_3-$BaCO_3$-based auxiliary layer (mp-Sensor), which was prepared by utilizing constituent metal acetates and polymethylmethacrylate microspheres as a template, showed faster CO_2 response and recovery and smaller cross-response against humidity changes than those obtained with a dense auxiliary layer without pores (d-Sensor). The magnitude of CO_2 response of mp-Sensor was slightly larger than the theoretical one, probably due to the existence of impurities which might have reacted with CO_2 in the auxiliary layer. On the other hand, c-Sensor with a thicker and dense auxiliary layer, which was prepared by commercially available carbonates, showed smaller CO_2 response and larger cross-response to humidity than mp-Sensor and d-Sensor. Thus, the use of the porous auxiliary layer prepared by constituent metal acetates was confirmed to be effective for improving the CO_2 sensing properties along with the large CO_2 response and small cross-response to humidity.

Keywords: CO_2 gas sensor; Solid-electrolyte; NASICON; Carbonate; Macropore; Humidity

1. Introduction

CO_2 gas is well-known as a typical greenhouse effect gas. The CO_2 concentration in the atmosphere increased steeply in the past quarter century, and the rise in global temperature and following sea-level rise are now serious issues in our world. In addition, CO_2 also affects human health [1]. On the other hand, the efficiency of photosynthesis of plants is largely dependent on the CO_2 concentration in the atmosphere, and an appropriate concentration has a positive effect on an increase in crop yields [2,3]. CO_2 concentration is generally measured by infrared-type sensors, but they cannot be used widely because of their large size and high cost. Therefore, development of low-cost portable CO_2 sensors with high sensitivity and selectivity is desired in various fields such as maintenance of living atmospheres and agricultural, biological and automobile industries. Some types of CO_2 gas sensors, such as resistive, optical, capacitive and solid electrolyte type, have been thus far studied eagerly by many researchers [3-9]. Electrochemical solid-electrolyte sensors attached with metal carbonates as an auxiliary layer atop the sensing electrode are very promising among them [6-9]. It was reported that some binary carbonates (e.g., Li_2CO_3-$BaCO_3$) as the auxiliary layer showed relatively high CO_2 sensing properties [10,11]. However, they have some

problems such as poor long-term stability [12] and large cross-sensitivity to water vapor [13,14]. Those problems have been studied and improved partially by mixing some metal oxides with the binary carbonates and by selecting the material of the counter electrode [13,15-17]. However, control of the macrostructure has not been investigated well in the field of solid-electrolyte gas sensors, except for a few works by Plashnitsa et al. [18,19]. On the other hand, we have so far succeeded to develop various high-potential gas sensors by introducing well-developed sub-micron size macropores into the sensing layer [20-25]. If such macroporous structure is introduced into the auxiliary phase of solid-electrolyte sensors, various sensing properties, such as humidity effect, response and recovery speeds and CO_2 response, are expected to be improved. Therefore, effects of introduction of macropores into the auxiliary layer of NASICON solid-electrolyte gas sensors were investigated in this study.

2. Experimental

2.1 Fabrication of sensor devices

Na^+ super ionic conductor (NASICON) powder was prepared from $Si(OC_2H_5)_4$, $Zr(OC_4H_9)_4$, $PO(OC_4H_9)_3$ and $NaOC_2H_5$ by a conventional sol-gel method [14]. They were mixed in an ethanol solvent kept at ca. 70ºC for 12 h with a small amount of nitric acid as a catalyst and ultrapure water under a N_2 flow, and then these alkoxides were hydrolyzed in the solution. The xerogel obtained was dried at 120ºC for 24 h and then heated at 750ºC for 1 h to remove organic compounds and to get the NASICON powder. The NASICON powder obtained was pressed into a disc (10 mm in diameter) and then sintered at 1100ºC for 5 h in air.

A pair of Au electrodes was deposited on the NASICON disc by ion sputtering and then heat-treated at 600ºC for 2 h in air. A polymethylmethacrylate (PMMA, 1.5 μm in diameter) template film was covered on one of two Au electrodes (sensing electrode) by dip-coating of an aqueous PMMA suspension containing a dispersant (P123: $((EO)_{20}(PO)_{70}(EO)_{20}$, MW: 5800, EO: ethylene oxide, PO: propylene oxide). Thereafter, the template was air-dried at room temperature, allowing the PMMA microspheres to self-assemble into a 3-D array by sedimentation. Subsequently, an aqueous 1.5 mol dm^{-3} acetate (CH_3COOLi:$Ba(CH_3COO)_2$ = 1:1 in molar ratio) solution as a precursor of binary carbonate (Li_2CO_3:$BaCO_3$ = 1:2 in molar ratio) was soaked into the template film, and dried in vacuo. The resultant film was fired at 500ºC for 1.5 h in air to decompose the PMMA template and to obtain a macroporous binary carbonate layer. The sensor with such a macroporous auxiliary layer will be referred to as mp-Sensor.

On the other hand, sensors with a dense auxiliary layer were also fabricated by the similar process, but without the PMMA template film. The thickness of the auxiliary layer was controlled by the number of dip-coating of the precursor acetate solution. For both mp-Sensor and d-Sensor, the thickness of the auxiliary layer was controlled to be the same.

Besides these sensors, a conventional sensor (c-Sensor) was fabricated using commercially

available carbonates (mean particle size: 0.7 ~ 1 μm) as raw materials for the auxiliary layer. A pair of Au electrodes of c-Sensor was only deposited by screen-printing of Au paste. Then, the binary carbonate paste, which contained Li_2CO_3 and $BaCO_3$ powders (Kishida Chemical Co., Ltd.) in α-terpineol (Li_2CO_3:$BaCO_3$ = 1:2 in molar ratio), was also screen-printed on one of two Au electrodes and fired at 600ºC for 2 h..

The binary carbonate powders obtained were characterized by X-ray diffraction analysis (XRD, Rigaku Corp., RINT 2000) and the microstructure of the auxiliary layers of all sensors was observed by a scanning electron microscope (SEM, Hitachi Ltd., S-2250).

2.2 Measurement of CO_2 sensing properties

Sensing properties to CO_2 of the sensors were measured at 400ºC by switching the atmosphere between 500 and 5000 ppm CO_2 balanced with a synthetic air at 30 min intervals. A difference between EMF in 500 ppm CO_2 (EMF_{500}) and that in 5000 ppm CO_2 (EMF_{5000}) was defined as a gas response ΔEMF_{CO_2} (EMF_{5000}-EMF_{500}) in the present study. In addition, an EMF shift induced by a humidity change from 0% to 70% relative humidity (RH), ΔEMF_{RH}, was measured. RH was controlled by mixing a dry air with a wet air containing saturated water-vapor at 25ºC; the wet air was prepared by bubbling the dry air through liquid water at 25ºC. The number of electrons involved with the electrochemical reaction on the sensing electrode was estimated from the EMF dependence on CO_2 concentration. 90% response and recovery times were represented by Res and Rec, respectively.

3. Results and Discussions

3.1 Characterization of auxiliary layers

Figure 1(a) shows an XRD pattern of grayish powder prepared from an aqueous CH_3COOLi and $Ba(CH_3COO)_2$ mixed solution by a sol-gel method, which was used for the auxiliary layers for mp- and d-Sensors. It is found that Li_2CO_3 and $BaCO_3$ existed as the main phases and there was no notable peaks ascribed to their oxides or hydroxides. Both Li_2CO_3 and $BaCO_3$ phases are known to exist individually at 400ºC, which was the operating temperature of the sensors in this study, as supported by the phase diagram for Li_2CO_3-$BaCO_3$ [26]. An XRD pattern of the white powder prepared from commercially available carbonates used for c-Sensor is shown in Fig. 1(b). It is almost comparable to that of the powder prepared from Li and Ba acetates, but the peaks ascribed to Li_2CO_3 were comparatively larger than those of the powder prepared from Li and Ba acetates.

SEM photographs of a PMMA template film fabricated on an Au electrode atop a NASICON disc are shown in Fig. 2. PMMA microspheres of 1.5 μm in diameter were closely packed on the substrate, as shown in Fig. 2(a). The thickness of the PMMA film was 10.0~11.5 μm with 8~9 layers of the PMMA microspheres which were uniformly stacked over each other, as shown in Fig. 2(b).

Unfortunately, a few and much smaller PMMA microspheres with a diameter less than 500 nm were mixed as a contaminant with the generally sized PMMA microspheres used in this study.

Figure 3 shows a porous Li_2CO_3-$BaCO_3$ binary carbonate film used as the auxiliary layer for mp-Sensor fabricated by utilizing the PMMA microsphere film as a template. Relatively uniform and well-developed porous structure with spherical macropores with a diameter of ca. 1.37 μm and a carbonate wall thickness of ca. 165 nm was observed on the surface of the auxiliary layer. The size of macropores was a little bit smaller than that of the PMMA microsphere templates (diameter: 1.5 μm). In addition, the cross-sectional view of the porous carbonate film showed that the bulk was also extremely porous, but the framework of macropores did not maintain the spherical morphology of PMMA microspheres. That is probably because the grain growth of the carbonates (especially Li_2CO_3) occurred even at 400ºC during the thermal decomposition of PMMA microspheres and acetates. The thickness of this porous carbonate film was approximately 6 μm.

SEM photographs of the auxiliary layers for d- and c-Sensors are shown in Fig. 4. Existence of a few small pores was confirmed on the surface of both layers, but the bulks were extremely dense for both cases. It is obvious that the carbonate grain of the dense auxiliary layer for d-Sensor is smaller (0.5 ~ 2.5 μm) than that for c-Sensor (8 ~ 10 μm), indicating reduced grain growth in the case of d-Sensor. Carbon residues produced by decomposition of Li and Ba acetates may have inhibited the grain growth of the carbonates in the case of d-Sensor. The thickness of the auxiliary layer for d-Sensor (ca. 6 μm, see Fig. 4(a)) was almost similar to that for mp-Sensor, while that for c-Sensor (ca. 11.5 μm, see Fig. 4(b)) was relatively thicker than others. The thicker auxiliary layer for c-Sensor was originated from its preparation method, i.e. the film less than 10 μm was hard to be fabricated by a conventional screen-printing method.

3.2 CO_2 sensing properties

Figure 5 shows response transients of all sensors to CO_2 gas under 0 and 70% RH at 400°C. Response and recovery speeds of mp-Sensor (Res: 85 s, Rec: 290 s) were much faster than those of d-Sensor (Res: 510 s, Rec: 710 s) at 0% RH. This is because CO_2 molecules easily diffused into the porous auxiliary layer for mp-Sensor, leading to quick adsorption and desorption of CO_2 on the reactive site (four-phase interface; solid electrolyte, Au electrode, carbonates and atmosphere) and then to quick equilibrium of a redox process containing CO_2 [15] as follows;

$$\text{Sensing electrode: } Li_2CO_3 = 2Li^+ + CO_2 + (1/2)O_2 + 2e^- \quad (1)$$

$$\text{Counter electrode: } 2Na^+ + 1/2\ O_2 + 2e^- = Na_2O \quad (2)$$

The ion exchange reaction shown below should occur at the interface, in order for the change of Na^+ activity to be brought about. Note that the activity of these oxides is not one.

$$Na^+ + Li_2O = Li^+ + Na_2O \quad (3)$$

In addition, a drastic increase of the reaction sites (four-phase interface) by the introduction of the macropores also provides the fast response and recovery speeds. As expected, response and recovery speeds of c-Sensor (Res: 225 s, Rec: 370 s) were comparable to those of d-Sensor, because of the dense auxiliary layers.

The magnitude of CO_2 response of mp-Sensor (ΔEMF_{CO_2}: 78.2 mV) was almost similar to that of d-Sensor (ΔEMF_{CO_2}: 78.9 mV) at 0% RH, but c-Sensor showed a small CO_2 response (ΔEMF_{CO_2}: 63.9 mV) in comparison with those of d-Sensor and mp-Sensor. The difference in ΔEMF_{CO_2} of these sensors will be discussed in relation with the morphology of these auxiliary layers in the following section. On the other hand, the difference in humidity between 0% and 70% RH did not influence the response and recovery speeds of all sensors, while ΔEMF_{CO_2} values at 70% RH of all sensors (e.g., 77.6 mV for mp-Sensor) were a little bit smaller than those at 0% RH (e.g., 78.2 mV for mp-Sensor). Therefore, H_2O molecules in the test atmosphere may have interrupted the adsorption of CO_2 molecules on the auxiliary layers. In addition, ΔEMF_{RH} for mp-Sensor (ca. 10 mV) was much smaller than those for d-Sensor (ca. 26 mV) and c-Sensor (ca. 35 mV) in 500 ppm CO_2. This behavior means that the magnitude of cross-response to humidity is affected by the bulk morphology of the auxiliary layer.

Response transients to humidity of mp-Sensor and d-Sensor were measured in 500 ppm CO_2 balanced with air at 400ºC, as shown in Fig. 6, in order to investigate the effect of the morphology of the auxiliary layer on the magnitude of cross-response to humidity. The magnitude of EMF of mp-Sensor (maximum ΔEMF_{RH}: 21.1 mV) increased abruptly, being accompanied with overshoot-like behavior, as soon as humidity was changed from 0% to 70%, and thereafter EMF became stable with a small total shift in EMF (ΔEMF_{RH}: 11.4 mV). On the other hand, d-Sensor showed a large and stable ΔEMF (32.8 mV) when the humidity was changed from 0% RH to 70% RH. Generally, it is reported that H_2O molecules largely influence the electrode potential of solid electrolyte-type gas sensors [13]. A part of the Au surface underneath the macroporous auxiliary layer of mp-Sensor is exposed undoubtedly to the atmosphere in comparison with that underneath the dense auxiliary layer of d-Sensor. This means that the amount of H_2O molecules adsorbed on the Au surface of mp-Sensor is considered to be very close to that of the uncovered counter Au electrode, in comparison to that covered with the dense auxiliary layer of d-Sensor. Therefore, ΔEMF_{RH} of mp-Sensor was considered to be smaller than that of d-Sensor. Meanwhile, the EMF-overshooting behavior of mp-Sensor, which was observed immediately after the humidity change from 0% to 70% RH, was suggested to arise from the difference in H_2O diffusivity to the carbonate-coated sensing and uncovered counter Au electrodes. Namely, it is thought that H_2O molecules rapidly adsorbed on the uncovered counter electrode in comparison with the sensing electrode covered with the binary carbonate layer, immediately after the humidity change from 0% to 70% RH, but the amount of H_2O molecules adsorbed on the sensing electrode became close to that on the counter electrode after several seconds. On the other hand, the diffusion of H_2O through the dense auxiliary layer was considered to be much slower than that through the porous auxiliary layer. Thus, the EMF-overshooting of the d-Sensor did not seem to occur. Also, the reason for the potential changes with RH is not identified clearly yet, but some electrochemical reaction with H_2O may relate to the

potential change.

3.3 Magnitude of CO_2 response

The response and recovery speeds of c-Sensor were so slow and comparable to those of d-Sensor, and ΔEMF_{RH} was larger than that of d-Sensor, probably because the auxiliary layer of c-Sensor was slightly denser and thicker than that of d-Sensor (see Fig. 4). In addition, ΔEMF_{CO_2} of c-Sensor (ca. 64 mV) was smaller than those of mp-Sensor and d-Sensor (ca. 78mV), as shown in Fig. 5. The number of electrons (*n*) can be estimated from the dependence of EMF on CO_2 concentration using the Nernst equation, derived from Eqs. (1) and (2), which is described as follows:

$$EMF = E^{\circ} + \frac{RT}{nF}\ln\left(\frac{a^{2}_{(s)Li^{+}} \times P_{(s)CO_2} \times a^{0.5}_{(s)O_2} \times a_{(c)Na_2O}}{a_{(s)Li_2CO_3} \times a^{2}_{(c)Na^{+}} \times a^{0.5}_{(c)O_2}}\right) \quad (4)$$

Here, E° is the standard cell potential depending on the free energy of reactions, R is the gas constant, T is the absolute temperature, *n* is the reaction number of electrons, F is the Faraday constant, and *a* is the activity. Subscripts mean reaction species on (s): sensing or (c): counter electrode, respectively.

The theoretical *n* value is 2.0, which is estimated from the general electrochemical reaction of this sensor (Eq. (1)). To measure exact *n* values, therefore, the dependence of EMF of mp-Sensor on CO_2 concentration was investigated in a CO_2 concentration range between 500 ppm and 5000 ppm, as shown in Fig. 7(a). The slope between EMF and the logarithm of CO_2 concentration showed n = 1.86 for mp-Sensor. The difference in *n* value between the theoretical and experimental values was obvious. Therefore, there is a possibility that some impurities in the auxiliary layer prepared from the aqueous acetate solution reacted with CO_2 molecules. As a matter of fact, the carbonate auxiliary layer of mp-Sensor was grayish after it was heated at 500ºC for 1.5 h in air containing 300 ppm CO_2 (as-prepared), as shown in Fig. 8 (a), while the color of binary carbonate (Li_2CO_3-$BaCO_3$) is usually white. On the other hand, after mp-Sensor was exposed to CO_2-free air at 400ºC for 50 h, the color of the auxiliary layer changed from gray to white just like ordinary carbonates, as shown in Fig. 8(b). The reaction electron number, *n*, of the sensor with this white carbonate auxiliary layer was 2.02 (see Fig. 7(b)), which was close to the theoretical n = 2. These results suggest that some impurities in the grayish auxiliary layer, which might have reacted with CO_2 gas, may have an influence on the reaction electron number. In addition, these impurities would not be the residues of PMMA, since such a deviation was observed not only with mp-Sensor but also with d-Sensor.

3.4 Effect of the thickness of a dense auxiliary layer on CO_2 sensing properties

Based on the above discussion, one may think that the sensor with a thinner dense auxiliary layer would show faster response and recovery behavior just like mp-Sensor, because such a film allows faster CO_2 diffusion nearby the Au sensing electrode. In contrast to our expectation, Salam et al. has

already reported that a thicker auxiliary layer improved various sensing properties such as CO_2 response speed, CO_2 sensitivity and long-term stability [27], while the auxiliary layer was Na_2CO_3 in their case. Therefore, we tried to investigate the effect of the thickness of a dense Li_2CO_3-$BaCO_3$ auxiliary layer fabricated from acetates on the CO_2 sensing properties in this study.

Figure 9 shows dependences of EMF_{500} and ΔEMF_{CO_2} under dry condition and ΔEMF_{RH} in 500 ppm CO_2 balanced with air on the thickness of the dense auxiliary layer of d-Sensor at 400ºC. All the auxiliary layers of d-Sensors tested were confirmed to be dense by SEM observation. For comparative purpose, the data obtained with mp-Sensor are also depicted in Fig. 9. Figure 9(a) shows that the EMF_{500} under dry condition monotonically decreases with an increase in the thickness of the dense auxiliary layer. The behavior of the dense Li_2CO_3-$BaCO_3$ auxiliary layer is similar to that of the Na_2CO_3 auxiliary layer [27]. In contrast, ΔEMF_{CO_2} under dry condition was smaller than the theoretical value, when the thickness of the auxiliary layer was less than 3 μm (Fig. 9(b)). The ΔEMF_{CO_2} markedly increased with an increase in the thickness of the dense auxiliary layer and beyond 3 μm it saturated to a level which was slightly higher than the theoretical value. It is reasonable to consider that the decreases of ΔEMF_{CO_2} for thinner auxiliary layers can be ascribed to a shortage of reaction species. Kida et al. demonstrated that the Li_2CO_3 in the auxiliary layer reacted with NASICON and a large amount of Li-components was released from the auxiliary layer to NASICON [28]. In the present case, the diffusion of Li-components might have occurred from the auxiliary layer to the solid electrolyte. So, the decrease in the amount of Li_2CO_3 in the auxiliary layer cannot be neglected in the case of thinner auxiliary layers. If a large amount of Li_2CO_3 was diffused away from the thin auxiliary layer, an activity of Li_2CO_3 will be decreased. This means a decrease of $a_{(s)Li_2CO_3}$ in the Nernst equation (4), leading to a larger EMF. In addition, the excessive loss of Li component decreases the activity, and the reaction with both Li^+ and Na^+ (Eq. (3)) does not occur smoothly. Thus, only EMF and ΔEMF of thinner auxiliary layers are considered to be affected by this phenomenon. Note that an EMF shift of about +80~90 mV was observed experimentally when CO_2 concentration was changed from 0 to 500 ppm CO_2, but the EMF was unstable. The experimental "0 ppm" actually corresponds to about 3 ppm CO_2 from Eq. (4). Therefore, the detection limit of CO_2 would be several ppm.

On the other hand, ΔEMF_{RH} in 500 ppm CO_2 balanced with air increased with an increase in the thickness of the auxiliary layer. Only ΔEMF_{RH} of d-Sensor with the thinnest layer (ca: 0.46 μm) was a negative value (ca. –4.9 mV), but a thinner auxiliary layer generally showed a smaller ΔEMF_{RH}, probably because of easier diffusion of H_2O molecules onto the Au electrode underlying the auxiliary layer, as in the case of the mp-Sensor discussed above. However, such a thinner auxiliary layer of d-Sensor resulted in an undesirably small ΔEMF_{CO_2} and a large EMF_{500} under dry condition. This dilemma can significantly be solved by introducing well-developed macroporous structure into the auxiliary layer. The data of mp-Sensor (open square symbols) in Fig. 9 showed a large ΔEMF and a small EMF_{500} comparable to those of d-Sensor with a thicker auxiliary layer and a small ΔEMF_{RH} comparable to that of d-Sensor with a thinner auxiliary layer. These results suggest that strict macrostructural control of an auxiliary layer for solid-electrolyte gas sensors is highly effective for improving the gas sensor properties.

4. Conclusions

A NASICON solid electrolyte-type CO_2 sensor using a macroporous auxiliary layer, mp-Sensor, showed faster response and recovery speeds to CO_2 as well as smaller ΔEMF_{RH} values than other two sensors using a dense auxiliary layer, d-Sensor and c-Sensor. mp-Sensor equipped with a porous auxiliary layer fabricated from Li and Ba acetates showed a larger CO_2 response than the theoretical one, but the response became theoretical after heat-treatment in CO_2-free air at 400ºC for 50 h.

d-Sensor with a thicker dense auxiliary layer showed much larger ΔEMF_{CO_2} and much smaller EMF_{500} values under dry condition than d-Sensor with a thin dense auxiliary layer. This behavior is probably caused by the diffusion of a large amount of Li^+ from the auxiliary layer to NASICON. On the other hand, a thinner auxiliary layer brought a much smaller cross-response to humidity, i.e. small ΔEMF_{RH} in comparison with a thicker dense auxiliary layer, because of easier diffusion of H_2O molecules onto the Au electrode underneath the auxiliary layer. More remarkable improvement in CO_2 sensing properties (large ΔEMF_{CO_2}, EMF_{500} in dry air, small ΔEMF_{RH}) could be achieved by an introduction of a macroprous structure into the auxiliary layer.

References

[1] D. S. Robertson, Health effect of increase in concentration of carbon dioxide in the atmosphere, Curr. Sci., 90 (2006) 1607-1609.

[2] L. J. Anderson, H. Maherali, H. B. Johnson, H. W. Polley and R. B. Jackson, Gas exchange and photosynthetic acclimation over subambient to elevated CO_2 in a C_3-C_4 grassland, Global Change Biology, 7 (2001) 693-707.

[3] A. Prim, E. Pellicer, E, Rossinyol, F. Peiró, A. Cornet and J. R. Morante, A novel mesoporous CaO-loaded In_2O_3 material for CO_2 sensing, Adv. Funct. Mater., 17 (2007) 2957-2963.

[4] K. Ertekin and S. Alp, Enhanced emission based optical carbon dioxide sensing in presence of perfluorochemicals (PFCs), Sens. Actuators B, 115 (2006) 672-677.

[5] T. Ishihara, K. Kometani, Y. Mizuhara and Y. Takita, Capacitive-type gas sensor for the selective detection of carbon dioxide, Sens. Actuators B, 13 (1993) 470-472.

[6] N. Miura, Y. Yan, M. Sato, S. Yao, S. Nonaka, Y. Shimizu and N. Yamazoe, Solid-state potentiometric CO_2 sensors using anion conductor and metal carbonate, Sens. Actuators *B*, 24-25 (1995) 260-265.

[7] P. Pasierb, S. Komornicki, S. Koziński, R. Gajerski and M. Rekas, Long-term stability of potentiometric CO_2 sensors based on Nasicon as a solid electrolyte, Sens. Actuators B, 101 (2004) 47-56.

[8] L. Wang, H. Zhou, K. Liu, Y. Wu, L. Dai and R. V. Kumar, A CO_2 gas sensor based upon composite Nasicon/Sr–β–Al_2O_3 bielectrolyte, Solid State Ionics, 179 (2008) 1662-1665.

[9] L. Wang and R. V. Kumar, A novel carbon dioxide gas sensor based on solid bielectrolyte, Sens.

Actuators B, 88 (2003) 292-299.

[10] S. Yao, Y. Shimizu, N. Miura and N. Yamazoe, Solid electrolyte CO_2 sensor using binary carbonate electrode, Chem. Lett., 19 (1990) 2033-2036.

[11] F. Qiu, L. Sun, X. Li, M. Hirata, H. Suo and B. Xu, Static characteristic of planar-type CO_2 sensor based on NASICON and with an inner-heater, Sens. Actuators B, 45 (1997) 233-238.

[12] M.Holzinger, J. Maier, W. Sitte, Fast CO_2-selective potentiometric sensor with open reference electrode, Solid State Ionics, 86-88 (1996) 1055-1062.

[13] Y. Miyauchi, G. Sakai, K. Shimanoe, N. Yamazoe, Fabrication of CO_2 sensor using NASICON thick film, Sens. Actuators B, 93 (2003) 250-256.

[14] T. Hyodo, T. Furuno, S. Kumazawa, Y. Shimizu amd M. Egashira, Effect of electrode materials on CO_2 sensing properties of solid-electrolyte gas sensors, Sens. Mater., 19 (2007) 365-376.

[15] H. Aono, Y. Itagaki and Y. Sadaoka, $Na_3Zr_2Si_2PO_{12}$-based CO_2 gas sensor with heat-treated mixture of Li_2CO_3 and Nd_2O_3 as an auxiliary electrode, Sens. Actuators B, 126 (2007) 406-414.

[16] Y. Miyachi, G. Sakai, K. Shimanoe and N. Yamazoe, Improvement of warming-up characteristics of potentiometric CO_2 sensor by using solid reference counter electrode, Sens. Actuators B, 108 (2005) 364-367.

[17] L. Satyanarayana, G. H. Jin, W. S. Noh, W. Y. Lee and J. S. Park, Influence of ceramic oxide materials on lithium based potentiometric CO_2 sensors, Curr. Appl. Phys., 7 (2007) 675-678.

[18] V. V. Plashinitsa, T. Ueda, and N. Miura, Improvement of NO_2 a sensing performances by an additional second component to the nano-structured NiO sensing electrode of a YSZ-based mixed-potential-type sensor, Int. J. Appl. Ceram. Technol., 3 (2006) 127-133.

[19] V. V. Plashnitsa, P. Elumalai, T. Kawaguchi and N. Miura, Zirconia-based sensor using impregnated nano-Au sensing electrode for selective detection of hydrocarbon, Proc. 12th Intern. Meeting on Chem. Sens., (2008) 332-333.

[20] T. Hyodo, K Sasahara, Y Shimizu and M. Egashira, Preparation of macroporous SnO_2 films using PMMA microspheres and their sensing properties to NO_x and H_2, Sens. Actuators B, 106 (2005) 580-590.

[21] H. Seh, T. Hyodo and H. L. Tuller, Bulk acoustic wave resonator as a sensing platform for NO_x at high temperatures, Sens. Actuators B, 108 (2005) 547-552.

[22] I.-D. Kim, A. Rothschild, T. Hyodo and H. L. Tuller, Microsphere templating as means of enhancing surface activity and gas sensitivity of $CaCu_3Ti_4O_{12}$ thin films, Nano Lett., 6 (2006) 193-198.

[23] Y. Takakura, T. Hyodo, Y. Shimizu and M. Egashira, Preparation of macroporous Eu-doped oxide thick films and their application to gas sensor materials, IEEJ Trans. SM, 128 (2008) 137-140.

[24] S. Nonaka, T. Hyodo, Y. Shimizu and M. Egashira, Preparation of macroporous semiconductor gas sensors and their odor sensing properties, IEEJ Trans. SM, 128 (2008) 141-144.

[25] K. Hieda, T. Hyodo, Y. Shimizu and M. Egashira, Preparation of porous tin dioxide powder by ultrasonic spray pyrolysis and their application to sensor materials, Sens. Actuators B, 133 (2008) 144-150.

[26] P. Pasierb, R. Gajerski, M. Rokita and M. Rekas, Studies on the binary system Li_2CO_3–$BaCO_3$,

Physica B, 304 (2001) 463-476.
[27] F. Salam, S. Bredikhin, P. Birke and W. Weppner, Effect of the thickness of the gas-sensitive layer on the response of solid state electrochemical CO_2 sensors, Solid State Ionics, 110 (1998) 319-325.
[28] T. Kida, H. Kawase, K. Shimanoe, N. Miura, N. Yamazoe, Interfacial structure of NASICON-based sensor attached with Li_2CO_3-$CaCO_3$ auxiliary phase for detection of CO_2, Solid State Ionics, 136-137 (2000) 647-653

Biographies

Masataka Morio received his BE degree in materials and engineering in 2005 from Nagasaki University. He is now a student in Graduate School of Science and Technology, Nagasaki University, and is currently engaged in research and development of a solid electrolyte type CO_2 gas sensor.

Takeo Hyodo received his BE degree in applied chemistry and ME degree in materials science and technology in 1992 and 1994, respectively, and DrEng degree in 1997 from Kyushu University. He has been a research associate at Nagasaki University since 1997. His current interests are the dev elopement of electrochemical devices such as chemical sensors and lithium batteries, and mesoporous and macroporous materials.

Yasuhiro Shimizu received his BE degree in applied chemistry in 1980 and DrE degree in 1987 from Kyushu University. He has been a professor at Nagasaki University since 2005. His current research concentrates on design of intelligent sensors by controlling gas diffusivity and reactivity, development of new sensor materials.

Makoto Egashira received his BE degree and ME degree in applied chemistry in 1966 and 1968, respectively, and DrEng degree in 1974 from Kyushu University. He has been a professor at Nagasaki University since 1985. His current interests include the development of new chemical sensors and surface modification of ceramics, preparation of hollow ceramic microspheres and porous films.

Figure captions

Fig. 1. XRD patterns of mixed Li_2CO_3-$BaCO_3$ binary powders prepared from (a) an aqueous CH_3COOLi and $Ba(CH_3COO)_2$ solution by a sol-gel method and (b) commercially available Li_2CO_3 and $BaCO_3$ powders.

Fig. 2. SEM photographs of a PMMA microsphere template film.

Fig. 3. SEM photographs of an auxiliary layer of mp-Sensor.

Fig. 4. SEM photographs of dense auxiliary layers of (a)-(c) d-Sensor and (d) and (e) c-Sensor.

Fig. 5. Response transients of (a) mp-Sensor, (b) d-Sensor and (c) c-Sensor to CO_2 under 0% RH and 70% RH at 400ºC. 90% response and recovery speeds of each sensor are indicated as Res and Rec respectively in the figure.

Fig. 6. Response transients of (a) mp-Sensor and (b) d-Sensor to humidity in 500 ppm CO_2 balanced with air at 400ºC.

Fig. 7 Variation of EMF with CO_2 concentration at 400ºC for mp-Sensor (a) as-prepared (gray carbonates) and (b) heat-treated at 400ºC for 50 h (white carbonates).

Fig. 8 Photographs of mp-Sensor (a) as-prepared and (b) after heat-treated at 400ºC for 50 h in CO_2-free air.

Fig. 9 Variations in (a) EMF_{500} and (b) ΔEMF_{CO_2} under dry condition and (c) ΔEMF_{RH} in 500 ppm CO_2 with the thickness of the auxiliary layer of d-Sensor. The data obtained with mp-Sensor are also plotted.

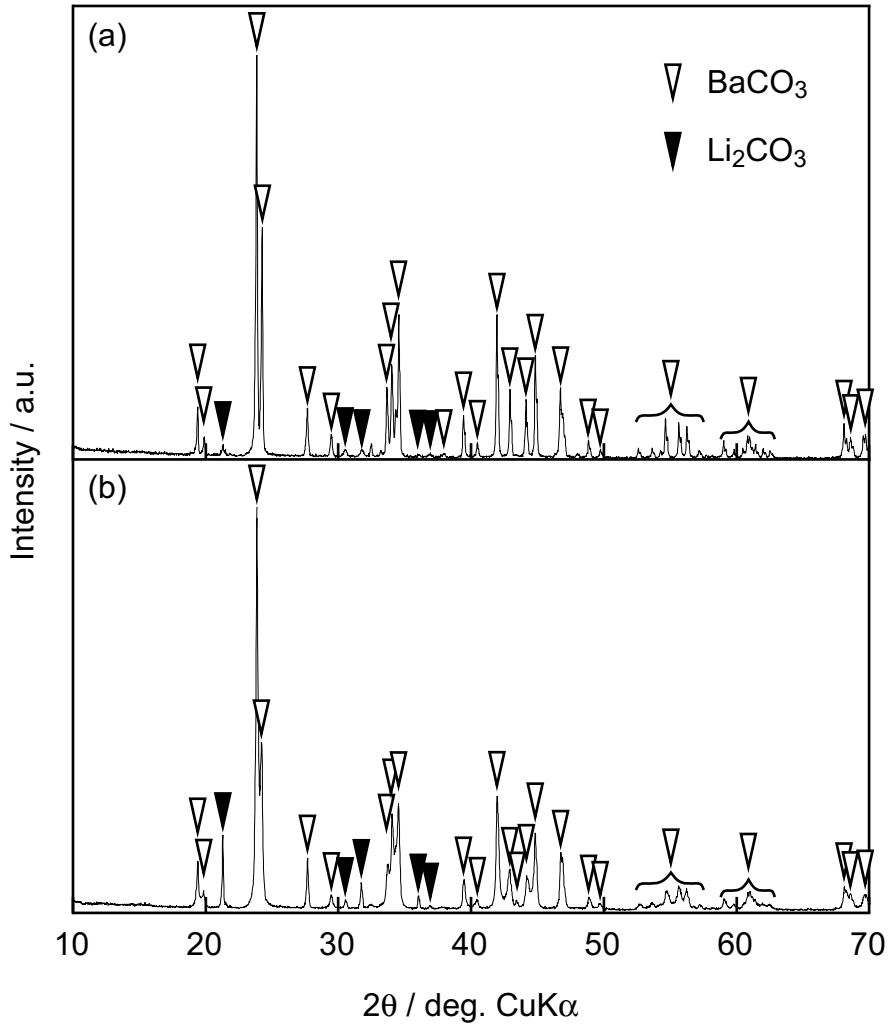

Fig. 1 Morio et al.

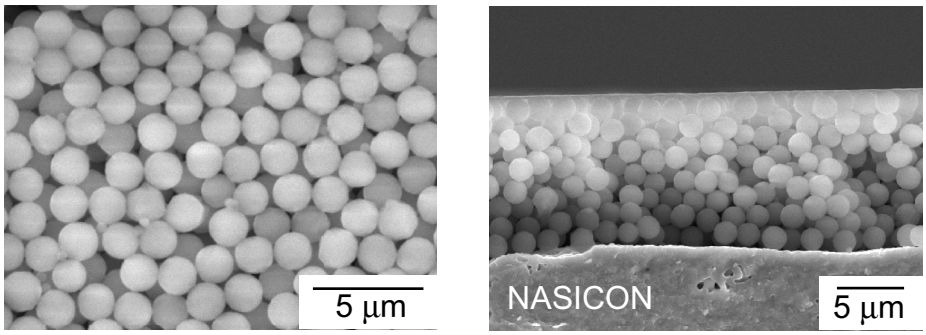

(a) Surface (b) Cross section

Fig. 2 Morio et al.

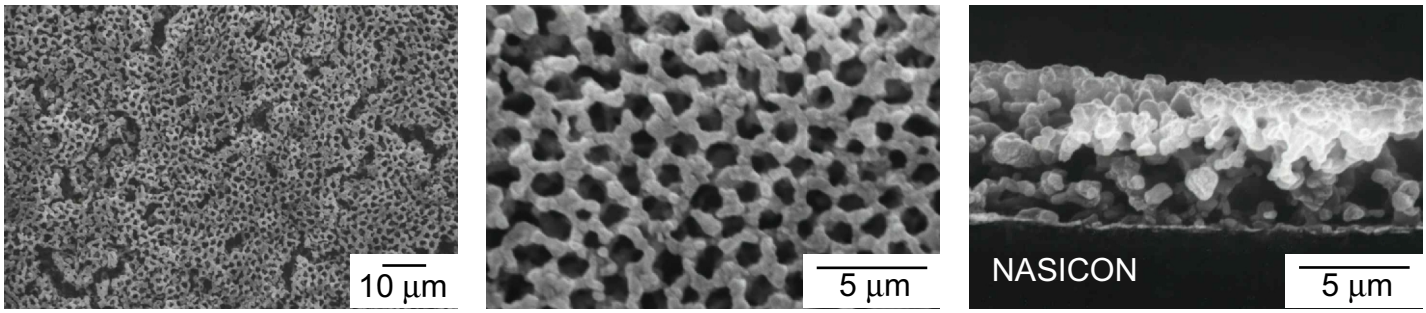

(a) Surface (b) Surface (c) Cross section

Fig. 3 Morio et al.

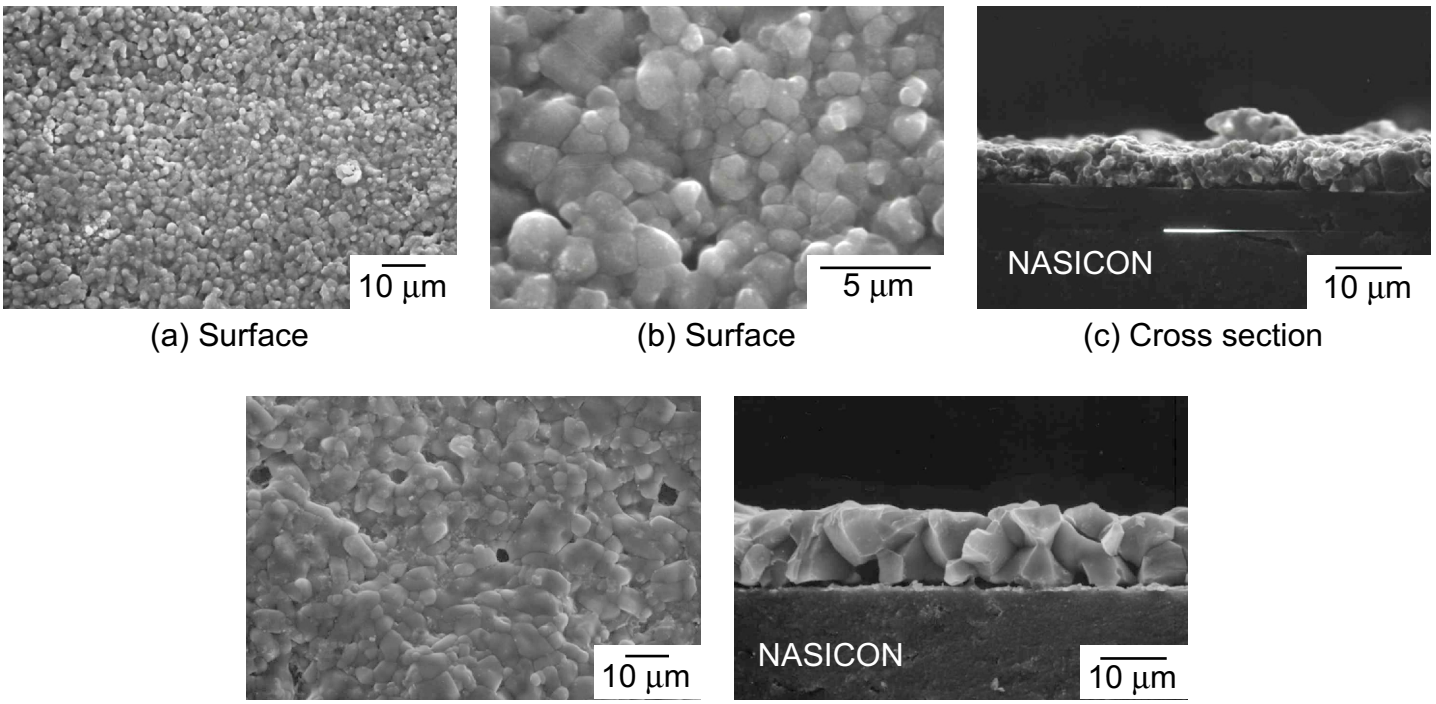

(a) Surface (b) Surface (c) Cross section

(d) Surface (e) Cross section

Fig. 4 Morio et al.

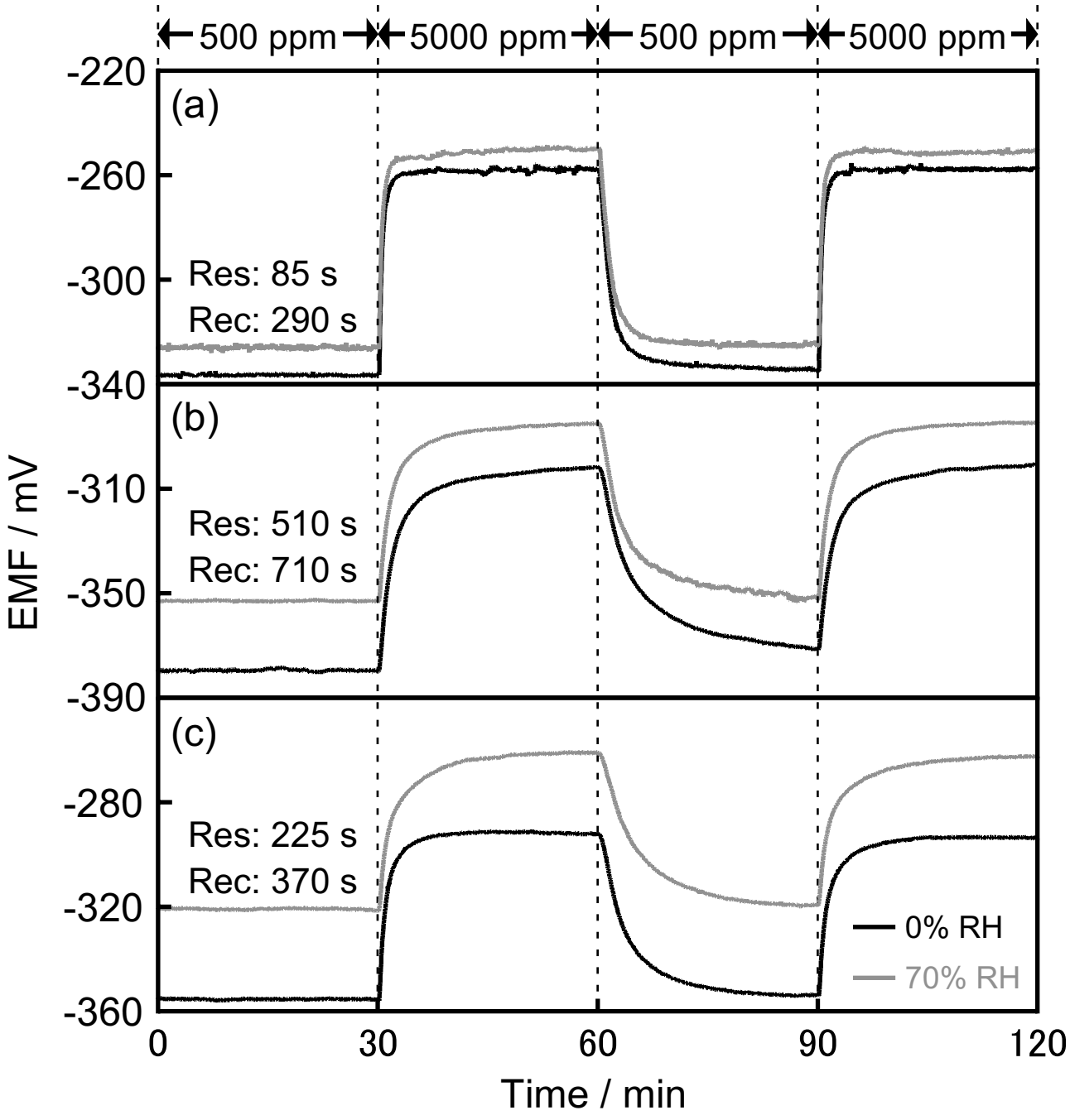

Fig. 5 Morio et al.

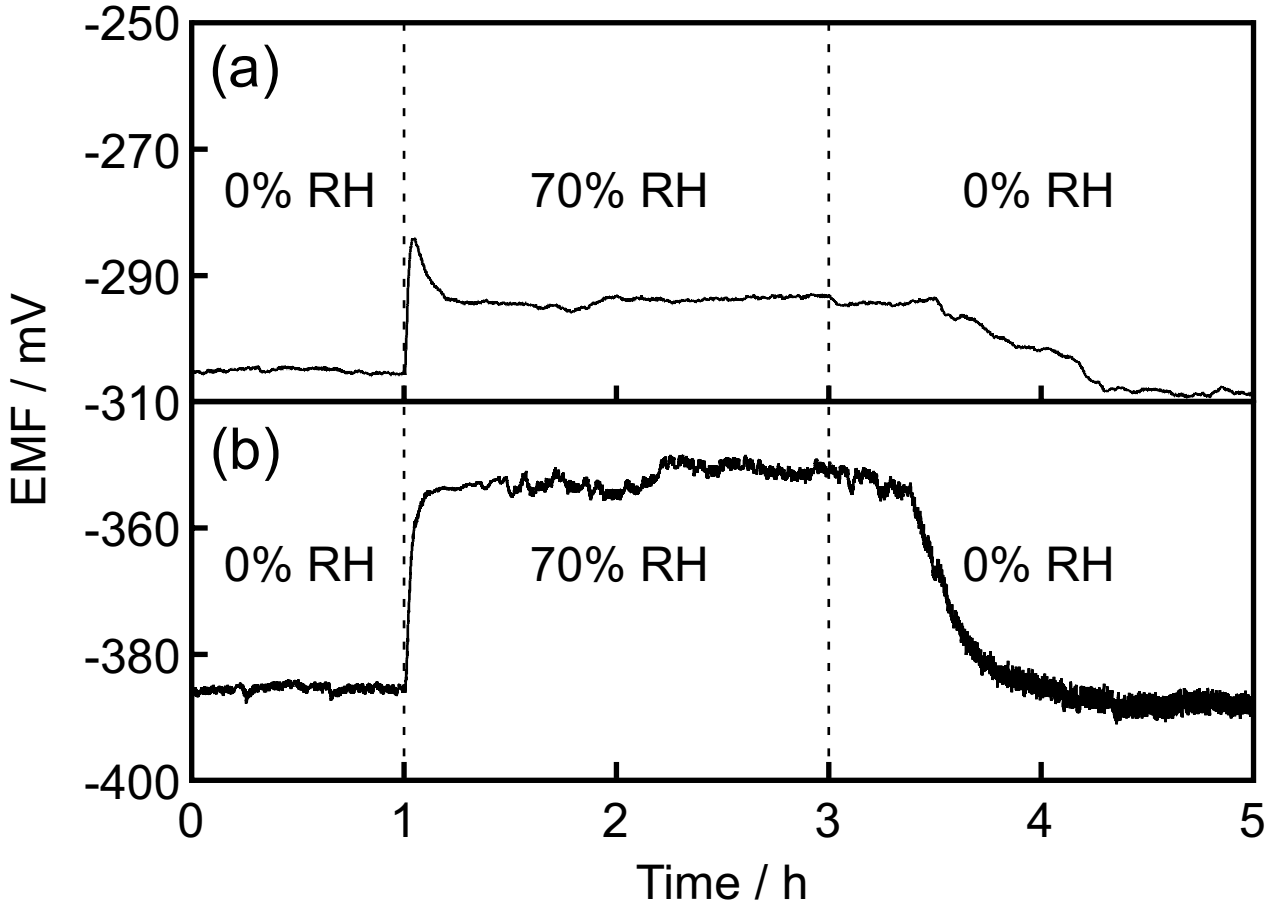

Fig. 6 Morio et al.

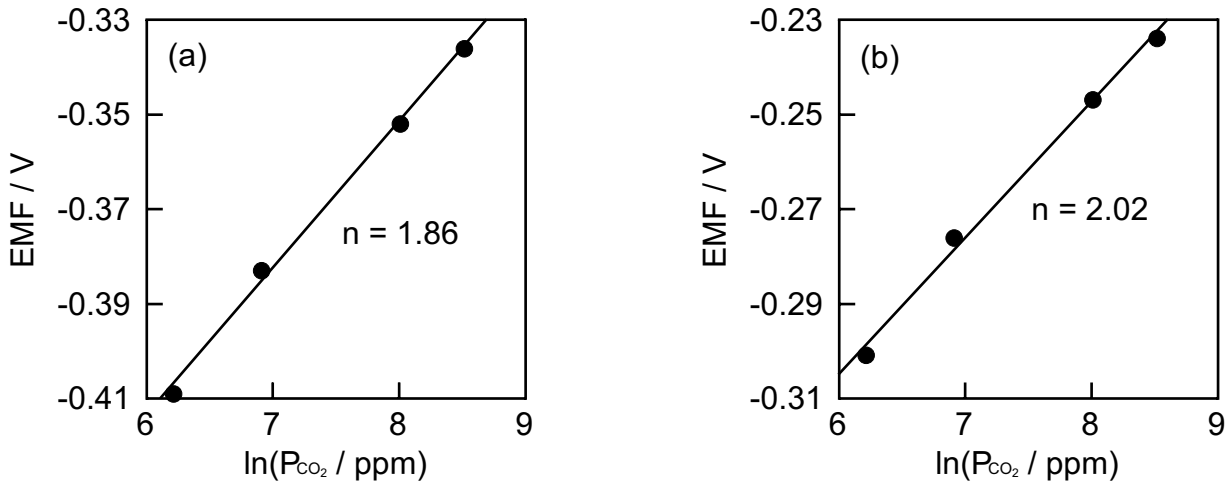

Fig. 7 Morio et al.

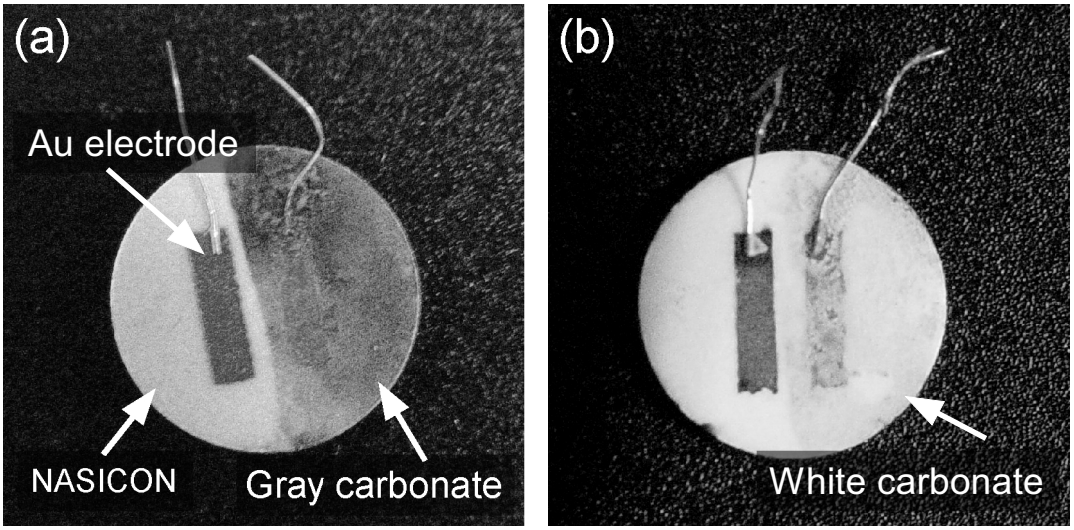

Fig. 8 Morio et al.

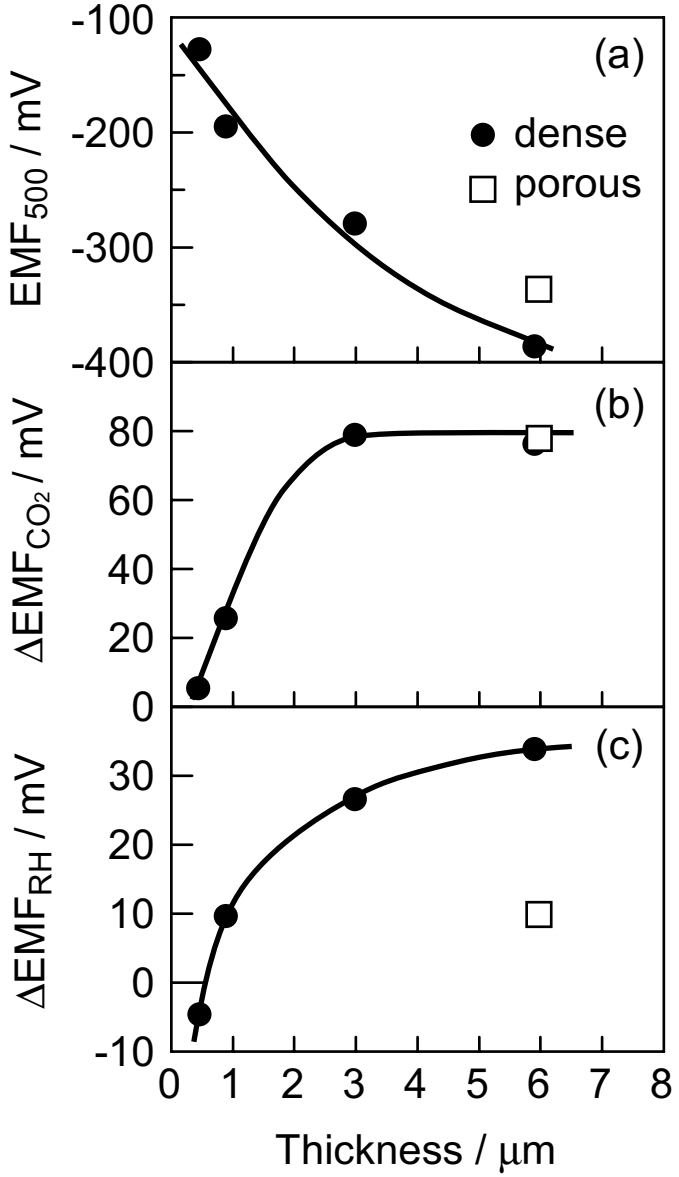

Fig. 9 Morio et al.